論 文 の 内 容 の 要 旨

論文題目　　　Development of Efficient and Semitransparent Perovskite Solar Cells by Nanooptical and Plasmonic Approaches

（ナノ光学およびプラズモニクスを利用した半透明ペロブスカイト太陽電池の開発と効率化）

氏　　名　　金　揆旼

**Introduction**

　　Semi-transparent solar cells would be applied to photovoltaic glasses and windows, which harvest light from both sides, as well as tandem cells. In case of perovskite solar cells (PVSCs), which attract growing attention recently, semi-transparent cells can be fabricated by decreasing the amount of the perovskite material in the cell [1]. However, it causes an efficiency drop because light absorption is reduced. In the present work, efficient and semi-transparent PVSCs are developed by smoothing the perovskite layer surface to suppress the light scattering, and enhancing excitation of the perovskite material, in particular at its absorption edge region, by using plasmonic nanostructures.

　　**Semitransparent PVSCs with ultrasmooth perovskite films.** A method called short spinning and vacuum drying (SSVD) was developed to produce ultrasmooth perovskite films. Fabrication process regarding SSVD is shown in Figure 1. Unlike other procedures for PVSCs, SSVD does not require humidity controlled environments such as a nitrogen glove box. The substrates processed by SSVD are visually transparent (Figure 2a, samples 1 and 3 with a
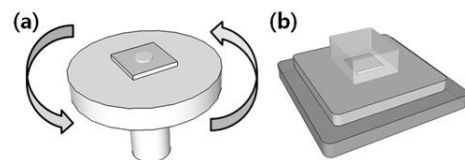


Figure 1. (a) Short spinning (SS) of a perovskite precursor ink within 5s and (b) prompt transfer of the substrate for vacuum drying (VD).

240- and 450-nm-thick perovskite layer, respectively). Interestingly, the 450-nm-thick perovskite layer processed by SSVD looks more transparent than a 300-nm-thick perovskite layer fabricated by a conventional method (Figure 2a, sample 2) despite the higher transmittance of the latter. The perovskite layers processed by SSVD have much lower surface roughness ($R_a \sim 6$ nm), suppressing light scattering at the surface (Figure 2b). The low scattering results in good visual transparency. These results reveal that not only transmittance but also scattering should be taken into account when dealing with visual transparency. In SSVD, exposure to moisture during spin-coating is minimized because of short spinning. Also, the perovskite precursor ink can be redistributed during the vacuum drying process, which fills the pin-holes on the surface. Thus smooth perovskite surfaces can be obtained.

Planar inverted PVSCs were fabricated by successive coating of PCBM, BCP, and silver on the ITO/PEDOT:PSS/perovskite substrate prepared by SSVD. The PCE value of 12.7 ± 1.6% (mean ± standard deviation) was achieved by the PVSC with a 240-nm-thick perovskite layer. PVSCs fabricated by SSVD did not show severe hysteresis during measurements of *J-V* characteristics, stemming from the highly smooth and ideal interface between the perovskite and BCP layers.

Taking advantage of the good visual transparency of the perovskite layers prepared by SSVD, semi-transparent PVSCs were also developed by introduction of a thin silver back electrode coated with $MoO_3$ (10 nm each). In the



Figure 2. (a) Transmittance and (b) scattering of ITO/PEDOT:PSS/perovskite samples fabricated by different methods.

semi-transparent PVSCs processed by SSVD, the thin back electrode shows extremely high smoothness ($R_a < 1$ nm) and low scattering, which result in good visual transparency. The semi-transparent PVSCs recorded the PCE of 10.7 ± 0.4% and 7.2 ± 1.5% with the 240-nm-thick perovskite layer and the PCE of 6.9 ± 0.4% and 5.1 ± 0.3% with 150-nm-thick perovskite layer for the front and back light irradiation. Unlike PVSCs with thick silver electrodes, the semi-transparent PVSCs show slight hysteresis depending on the scan rate mostly when the perovskite layer is thinner than 150 nm, which can be explained by unbalanced mobilities between the holes and the electrons [2].

**Efficiency enhancement of PVSCs by electrode-coupled plasmons.** Next the plasmonic enhancement [3] is applied to the PVSCs. Although Ag nanocubes (AgNCs) are suitable for the plasmonic enhancement because of their strong far-field scattering and intense optical near-field [4], their intrinsic resonant wavelength is too short to enhance the absorption of a perovskite film at its absorption edge region. To address this issue, film-coupled plasmons based on plasmon coupling between a MNP
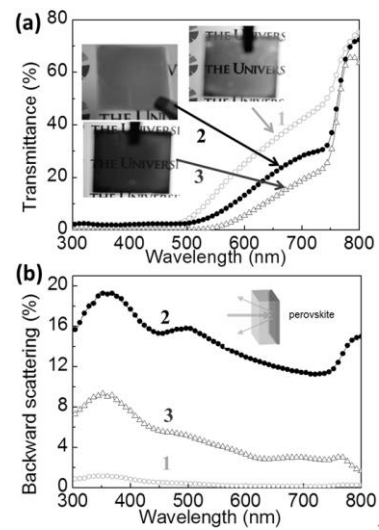
and a metal film [5] are exploited. The resonant wavelength is red-shifted by the coupling, and the wavelength can be controlled by tuning the gap between the MNP and the film. In this work, AgNCs are introduced in between the PCBM and BCP layers for three-dimensional coupling between the AgNCs and the silver electrode at the 5 faces (Figure 3b, inset), different from the conventional film-coupled
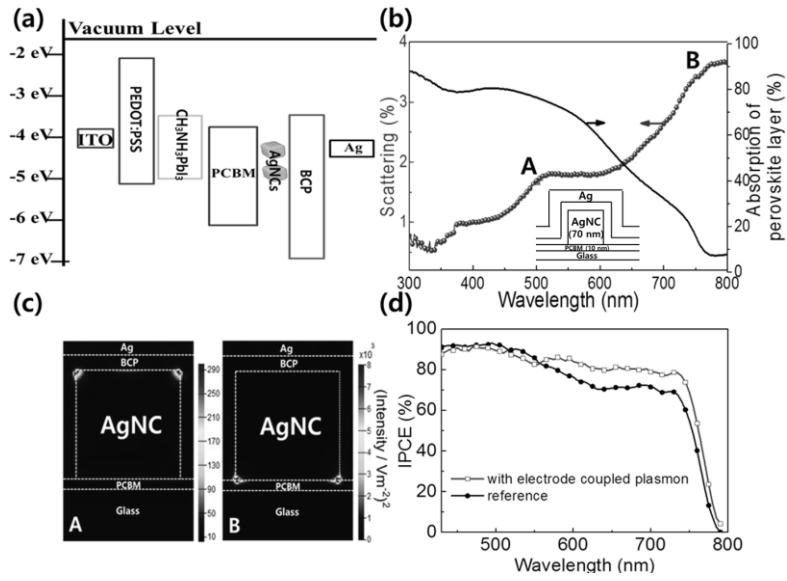


Figure 3. (a) Energy diagram of PVSCs with electrode-coupled plasmons. (b) Absorption of the perovskite layer and plasmonic scattering of the substrate depicted in the inset. (c) Electric field distributions for peaks A and B in (b). (d) IPCE of the PVSCs with and without electrode-coupled plasmons.

plasmons only at the bottom of MNP with a flat metal layer. The overall energy diagram and the structure of the cell are shown in Figure 3a. The resonant peak positions of the "electrode-coupled plasmons" are tuned by the size of AgNCs and the thickness of BCP layer.

On the basis of FDTD simulation, the AgNC size and the BCP layer thickness were optimized to be 70 nm and 10 nm, respectively, considering adjustment of the scattering peak to the absorption edge region of the perovskite layer and the high plasmonic scattering to plasmonic absorption ratio. Figure 3b shows the experimentally obtained scattering spectrum of electrode-couple plasmons with 70 nm of AgNCs and 10 nm of BCP. The plasmonic peak B is located near the absorption edge of the perovskite layer. We also simulated the electric field distributions for peaks A and B (Figure 3c). The electric fields are localized at the bottom side of AgNC for peak B, while those are confined between the upper side of AgNC and the electrode for peak A. Thus, peak B from electrode-coupled plasmons is expected to have a great impact on PVSCs to improve PCE.

To confirm this, PVSCs with electrode-coupled plasmonic structure were prepared. Their performances were largely dependent on the amounts and uniformity of AgNCs on PCBM. The PVSCs with 2% coverage of AgNCs showed the best PCE of $13.3 \pm 1.1\%$, while the value of PVSCs without AgNCs was $11.9 \pm 0.9\%$. The increase in PCEs mainly comes from the photocurrent improvement from $19.5 \pm 0.5$ to $21.4 \pm 0.5$ mA cm$^{-2}$. The photocurrents were improved near the absorption edge of the perovskite layer, confirmed from the IPCE action spectra (Figure 3d), indicating that the electrode-coupled plasmons enhanced the photocurrents.

**Introduction of electrode-coupled plasmons into semi-transparent PVSCs.** Electrode-coupled plasmons were also applied to the semi-transparent PVSCs, whose structure is shown in Figure 4a. The semi-transparent PVSCs with electrode-coupled plasmons using 2% coverage of AgNCs do not severely affect visual transparency compared to the cells without AgNCs as shown in Figure 4b. The semi-transparent PVSCs with 180-nm-thick perovskite layer with electrode-coupled plasmons showed higher photocurrents (15.9 mA



Figure 4. (a) Structure of the semi-transparent PVSC with electrode-coupled plasmons. (b) Visual images, (c) *J-V* curves, and (d) IPCE of the semi-transparent PVSCs with and without electrode-coupled plasmons.

cm$^{-2}$) compared to the cells without AgNCs (13.8 mA cm$^{-2}$) (Figure 4c). The IPCE data in Figure 4d show that this improvement results from the increase in the photocurrents in the whole visible range. Since this could be due to relatively weak coupling between the AgNCs and the thin electrode, further optimization of the parameters such as the AgNC size and the BCP layer thickness might be necessary for the photocurrent enhancement particularly in the absorption edge region of the perovskite layer.

**Conclusions**

In this research, SSVD method to fabricate ultrasmooth perovskite layers was developed, and applied to fabrication of semi-transparent PVSCs with suppressed scattering. Nanostructures exhibiting electrode-coupled plasmons were also proposed, and their tunability of the resonant wavelength and plasmonic enhancement effects on PVSCs were demonstrated experimentally. The photocurrents were enhanced particularly in the absorption edge region of the perovskite layer. The electrode-coupled plasmons were also exploited for photocurrent enhancements of the semi-transparent PVSCs. The work is currently underway toward generalization of the electrode-coupled plasmons with MNPs of different sizes and morphologies, so as to develop semi-transparent PVSCs with higher transparency and different colors.

**References**

1) G. E. Eperon, V. M. Burlakov, A. Goriely, and H. J. Snaith, *ACS Nano* **2014**, 8, 591.

2) C. S. Ponseca, T. J. Savenije *et al.*, *J. Am. Chem. Soc*. **2014**, 136, 5189.

3) H. A. Atwater and A. Polman, *Nat. Mater.* **2010**, 9, 205.

4) T. Kawawaki, H. Wang, T. Kubo, K. Saito, J. Nakazaki, H. Segawa, and T. Tatsuma, *ACS Nano* **2015**, 9, 4165.

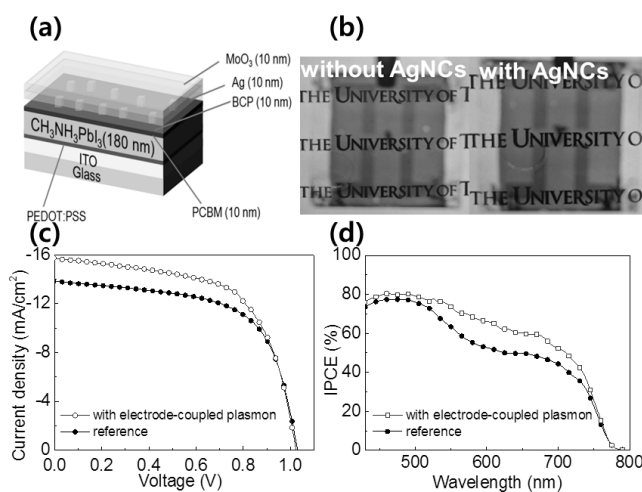5) J. J. Mock, R. T. Hill, A. Degiron, S. Zauscher, A. Chilkoti, and D. R. Smith, *Nano Lett.* **2008**, 8, 2245.